

A new switching look-up table for direct power control of grid connected 3L-NPC PWM rectifier

Azziddin M. Razali¹, Nor Azizah Yusoff², Kasrul Abdul Karim³, Auzani Jidin⁴, Tole Sutikno⁵

^{1,2,3,4}Faculty of Electrical Engineering, Universiti Teknikal Malaysia Melaka, Malacca, Malaysia

⁵Department of Electrical Engineering, Universitas Ahmad Dahlan, Yogyakarta, Indonesia

⁵Embedded System and Power Electronics Research Group, Yogyakarta, Indonesia

Article Info

Article history:

Received May 9, 2021

Revised Jul 1, 2021

Accepted Jul 27, 2021

Keywords:

Active and reactive powers

AC-to-DC converter

Direct power control

Multilevel PWM rectifier

Neutral point clamped

Multilevel converter

Switching look-up table

ABSTRACT

This paper presents a comprehensive and systematic approach in developing a new switching look-up table for direct power control (DPC) strategy applied to the three-phase grid connected three-level neutral-point clamped (3L-NPC) pulse width modulated (PWM) rectifier. The term of PWM rectifier used in this paper is also known as AC-DC converter. The approach provides detailed information regarding the effects of each multilevel converter space vector to the distribution of input active and reactive power in the converter system. Thus, the most optimal converter space vectors are able to be selected by the switching look-up table, allowing smooth control of the active and reactive powers for each sector. In addition, the proposed DPC utilizes an NPC capacitor balanced strategy to enhance the performance of front-end AC-DC converter during load and supply voltage disturbances. The steady state as well as the dynamic performances of the proposed DPC are presented and analyzed by using MATLAB/Simulink software. The results show that the AC-DC converter utilizing the new look-up table is able to produce almost sinusoidal line currents with lower current total harmonic distortion, unity power factor operation, adjustable DC-link output voltage and good dynamic response during load disturbance.

This is an open access article under the [CC BY-SA](https://creativecommons.org/licenses/by-sa/4.0/) license.



Corresponding Author:

Azziddin Mohamad Razali

Faculty of Electrical Engineering

Universiti Teknikal Malaysia Melaka (UTeM)

76100 Durian Tunggal, Malacca, Malaysia

Email: azziddin@utem.edu.my

1. INTRODUCTION

Research of multilevel pulse width modulation (PWM) converters are attracting much more attentions recently, due to its ability to be implemented in high power medium voltage applications. The use of multilevel converter allows the power conversion to be performed in smaller voltage steps in such a way the voltage stress in each semiconductor switch is reduced [1], [2]. With proper control strategy, a multilevel topology can be operated as the front-end rectifier which is able to be operated with lower switching losses and higher voltage capability. In addition, multilevel rectifier allows a reduction of the line current harmonics, reduced ac filter size and provide almost unity power factor operation [3]. The three-level neutral point clamped (3L-NPC) rectifier has a significant role in high power application due to the minimal devices it requires compared with other multilevel topologies [4]. However, there are a few inherent challenges exist in this topology such as the voltage drifts and voltage ripples of the neutral-point which limit its practical applications. In addition, the redundant switching states offered by 3L-NPC will create an issue to select the most effective voltage vectors which will improve the converter control system performance [5], [6].

Although the NPC topology offers numerous advantages, it reveals technical difficulties that complicate its real implementation [7], [8]. With 27 possible choices for voltage selection in 3L-NPC compared with only 8 in conventional 2L converter, the switching table in 3L-NPC becomes more complex compared with 2L topologies. However, NPC offers much more option of the voltage vector selection to satisfy the commutation condition. Another challenge in NPC is unbalance voltage in the neutral-point of DC-link capacitor [9]. This unbalance voltage may generate excessively large voltage in the respective switching devices which will deteriorate the overall converter system performance. In order to overcome the complexity of designing an effective switching look-up table, this paper presents a comprehensive and systematic approach in developing a new switching table for grid connected three-phase 3L-NPC AC-DC converter (rectifier). This is obtained by differentiating the active and reactive power equations. In this way, the switching table is able to choose the best converter voltage vector in order to ensure smooth control of instantaneous active and reactive powers during each of twelve sectors. In addition, a method to minimise the neutral-point voltage deviation is also discussed in this work.

2. DIRECT POWER CONTROL OF 3L-NPC PWM RECTIFIER

There are several variations of the direct power control (DPC) technique have been reported such as virtual flux DPC (VF-DPC) [10]-[14], predictive control DPC (P-DPC) [15], [16] and space vector modulation DPC (SVM-DPC) [19]-[21], implemented in a conventional 2L three-phase PWM AC-DC converter. However, the multilevel AC-DC converters appear to be a very good solution for medium and high power applications such as in wind energy, static compensator (STATCOM), back-to-back ac drives and high voltage direct current (HVDC) applications where adjustable DC-link output voltage, almost sinusoidal input line currents with low THD and adjustable power factor operation are required [22]. The use of such multilevel topology allows power level to be increased by adding more voltage levels in such a way the voltage stress in each semiconductor device is reduced 3L-NPC AC-DC converter has several advantages over the traditional 2L converter such as the former produces better quality output voltage and current waveforms with minimal voltage stress at each power switches [23]. The converters utilizing those DPC methods are able to produce almost sinusoidal line currents and unity power factor operation. The three-phase supply voltage and current are measured to estimate the instantaneous active P_{inst} and reactive powers Q_{inst} . Meanwhile, the reference active power P_{ref} is produced by multiplying the DC-link output voltage V_{DC} with the output from the PI controller while the reference reactive power Q_{ref} is set to zero in order to demonstrate a unity power factor operation. Subsequently, the command active power P_{ref} and reactive power Q_{ref} value are subtracted with calculated active and reactive power to produce the instantaneous active power error and reactive power error denoted by ΔP and ΔQ respectively. The error signals are processed by two hysteresis controllers to produce the power error status signals shown by dP and dQ in Figure 1.

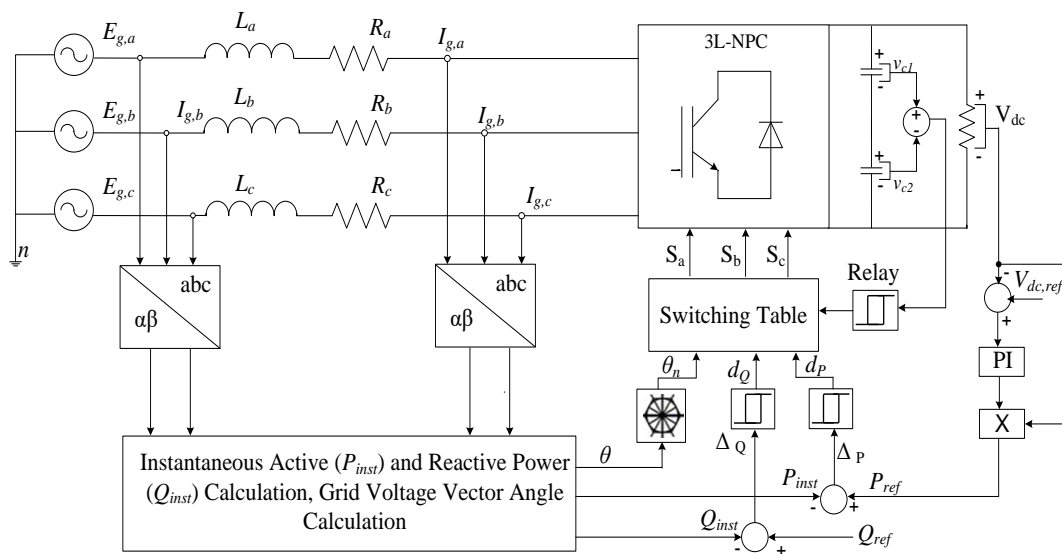


Figure 1. Block diagram of the DPC strategy for 3L-NPC rectifier

Figure 2 shows the topology of a grid-connected 3L-NPC rectifier with an L-type filter. The converter consists of twelve switching cells and six clamp diodes. Any given output phases of the converter can be connected to the negative ($S_{a1}=0, S_{a2}=0$), neutral ($S_{a1}=0, S_{a2}=1$), or positive ($S_{a1}=1, S_{a2}=1$) points of the DC-link, which results in a different current path between the DC side and ac side. The redundant switching states produced by the 3L-NPC rectifier create substantial issues in developing an effective switching table that can improve the DPC system performance [24].

Therefore, one of the NPC rectifier’s main tasks is to balance the upper and lower capacitor voltages. The imbalance of upper and lower capacitor voltages (v_{c1} and v_{c2}) may occur due to the application of short amplitude of voltage vectors. Each of the short amplitude of the voltage vector (inner hexagon) consists of double switching states as shown in Figure 3. The switching states are divided into P -type and the other is N -type. Both types of switching states have different effects on the capacitor voltage. The application of the P -type switching state will decrease the lower capacitor, v_{c2} while the N -type will increase the upper capacitor voltage, v_{c1} . The problem of capacitor voltage imbalance is necessary to be addressed for preventing a short circuit that produces system instability, high switching loss, and high dv/dt [25]. Hence, to ensure satisfactory performance and reliability of the three-level PWM rectifier, voltages across the two DC-link capacitors must be kept balanced.

Therefore, the attempts to optimize the selection of switching state for the short amplitude of voltage vector are depending upon the type of P -type and N -type to ensure the balancing between both capacitors. This balancing strategy is simple as it detects the increasing or decreasing of v_{c1} and v_{c2} by using a two-level hysteresis controller as the input is the error of two capacitor voltages. By using the information of increasing or decreasing of v_{c1} and v_{c2} , the hysteresis controller produces two outputs which are known as balancing status.

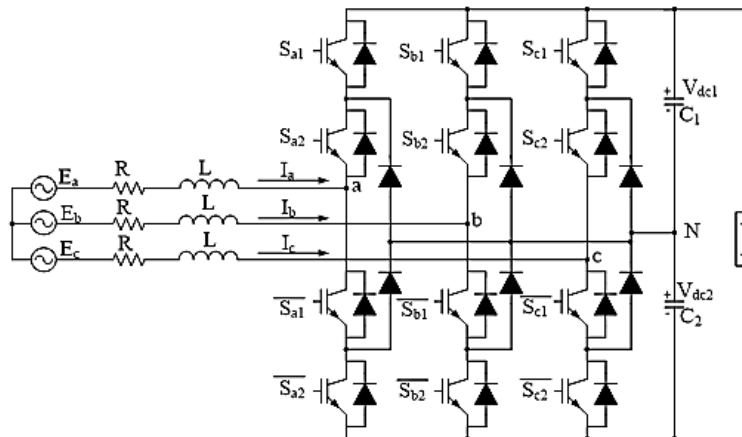


Figure 2. Topology of the 3L-NPC rectifier

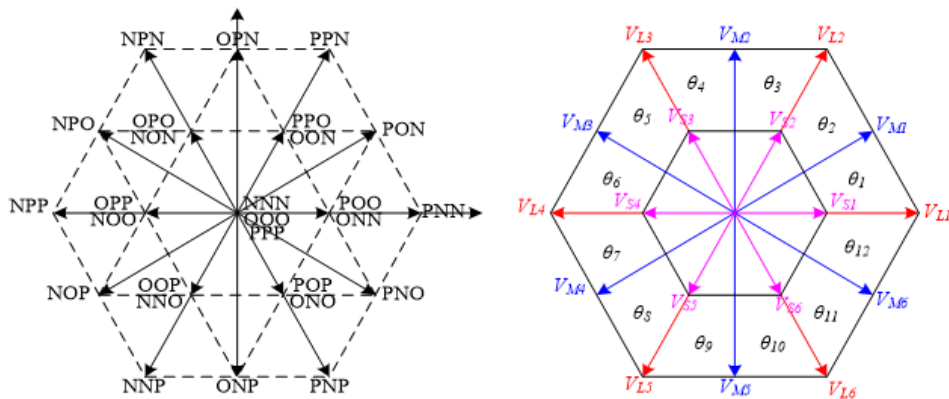


Figure 3. Space voltage vector of the 3L-NPC rectifier

3. DEVELOPMENT OF SWITCHING LOOK-UP TABLE FOR 3L-NPC DPC

The DPC is based on the direct torque control (DTC) concept in electrical machines. The intention for DPC is to control the instantaneous of active and reactive power control loops [10] as the same direction for DTC in controlling the torque and flux of induction machines. The proposed new switching look-up table is developed based on the differentiation of instantaneous active and reactive powers method. The instantaneous input active and reactive power of the front-end three-phase ac to DC converter in a stationary $\alpha\beta$ -reference frame is given by (1) and (2).

$$P_{inst} = \frac{3}{2}(E_{\alpha}I_{\alpha} + E_{\beta}I_{\beta}) \quad (1)$$

$$Q_{inst} = \frac{3}{2}(E_{\beta}I_{\alpha} - E_{\alpha}I_{\beta}) \quad (2)$$

Assuming that the system shown in Figure 1 is a balanced three-phase power system, the following converter per-phase equations related to the neutral-point of the grid can be derived.

$$V_{conv,an} = sw_{a1} \cdot V_{dc1} + sw_{a2} \cdot V_{dc2} \quad (3)$$

$$V_{conv,bn} = sw_{b1} \cdot V_{dc1} + sw_{b2} \cdot V_{dc2} \quad (4)$$

$$V_{conv,cn} = sw_{c1} \cdot V_{dc1} + sw_{c2} \cdot V_{dc2} \quad (5)$$

where:

$$sw_{a1} = \frac{2S_{a1} - (S_{b1} + S_{c1})}{3} \quad sw_{a2} = \frac{2S_{a2} - (S_{b2} + S_{c2})}{3} \quad (6)$$

$$sw_{b1} = \frac{2S_{b1} - (S_{a1} + S_{c1})}{3} \quad \text{and} \quad sw_{b2} = \frac{2S_{b2} - (S_{a2} + S_{c2})}{3} \quad (7)$$

$$sw_{c1} = \frac{2S_{c1} - (S_{a1} + S_{b1})}{3} \quad sw_{c2} = \frac{2S_{c2} - (S_{a2} + S_{b2})}{3} \quad (8)$$

The active and reactive power differentiations are calculated as (9) and (10).

$$\frac{dP}{dt} = \frac{3}{2} \left[E_{\alpha} \left(\frac{dI_{\alpha}}{dt} \right) + I_{\alpha} \left(\frac{dE_{\alpha}}{dt} \right) + E_{\beta} \left(\frac{dI_{\beta}}{dt} \right) + I_{\beta} \left(\frac{dE_{\beta}}{dt} \right) \right] \quad (9)$$

$$\frac{dQ}{dt} = \frac{3}{2} \left[E_{\beta} \left(\frac{dI_{\alpha}}{dt} \right) + I_{\alpha} \left(\frac{dE_{\beta}}{dt} \right) - E_{\alpha} \left(\frac{dI_{\beta}}{dt} \right) - I_{\beta} \left(\frac{dE_{\alpha}}{dt} \right) \right] \quad (10)$$

The equation for the grid voltage in the $\alpha\beta$ -stationary frame can be expressed in (11) by assuming the system in balance conditions

$$E_{\alpha} = E_s \cos(\omega t) \text{ and } E_{\beta} = E_s \sin(\omega t) \quad (11)$$

Based on the voltage equations of the grid-connected AC-DC converter as shown in, the instantaneous current variations can be expressed as (12) and (13).

$$\frac{dI_{g,\alpha}}{dt} = \frac{1}{L} (E_{g,\alpha} - V_{conv,\alpha} - I_{g,\alpha}R) \quad (12)$$

$$\frac{dI_{g,\beta}}{dt} = \frac{1}{L} (E_{g,\beta} - V_{conv,\beta} - I_{g,\beta}R) \quad (13)$$

The final derivatives equations for the active and reactive power in (14) and (15) can be obtained by neglecting the small value of the line resistance.

$$\frac{dP}{dt} = \frac{3}{2} \left[\omega E_{\alpha} I_{\beta} - \omega E_{\beta} I_{\alpha} + \frac{1}{L} (E_{\alpha}^2 - E_{\alpha} V_{conv,\alpha}) + \frac{1}{L} (E_{\beta}^2 - E_{\beta} V_{conv,\beta}) \right] \quad (14)$$

$$\frac{dQ}{dt} = \frac{3}{2} \left[\omega E_{\alpha} I_{\alpha} + \omega E_{\beta} I_{\beta} + \frac{1}{L} (E_{\alpha} E_{\beta} - E_{\beta} V_{conv,\alpha}) - \frac{1}{L} (E_{\alpha} E_{\beta} + E_{\alpha} V_{conv,\beta}) \right] \quad (15)$$

As can be seen in the in (9) and (10) respectively, the power derivatives are determined by the grid voltage, line current, and converter poles voltage in the $\alpha\beta$ -stationary frame. Then, the differentiation of active and reactive power as shown in (14) and (15) are plotted by implementing the required parameter for the AC-DC converter as shown in Table 1.

Table 1. Electrical Parameters of Power Circuit

Parameters	Value
Input phase voltage (peak), E_g	70.71 V
Source Voltage frequency, f	50 Hz
DC-link volatage reference, $V_{DC,ref}$	150 V
Resistance of reactance, R	0.2 Ω
Inductance of reactance, L	11 mH
DC-link capacitor, C	10.8 mF
Load Resistance, R_L	140 Ω
Sampling time, t_s	20 μ s

The illustration of the plotted waveform is shown in Figure 4 for the active power, and Figure 5 for the reactive power are adopt to subject the response of an instantaneous of active and reactive power towards the particular converter voltage vector, V_n . Therefore, to generate the most compatible lookup table, the response of the sign and magnitude acquiring in each sector has been implemented due to the change of active and reactive power. For example, for the angle in the range 0° to 30° , the application of short voltage vectors ($V_{S,3}$ $V_{S,4}$ $V_{S,5}$ $V_{S,6}$), medium voltage vectors ($V_{M,3}$ $V_{M,4}$ $V_{M,5}$), long voltage vectors ($V_{L,3}$ $V_{L,4}$ $V_{L,5}$), and zero voltage vectors (V_0 V_7) capable to produced for positive time-derivative for the active power. Thus, the active power tends to increase while those vectors are applied. However, through the implementation of voltage vector ($V_{S,1}$) from short, medium ($V_{M,6}$ $V_{M,1}$), and long ($V_{L,1}$ $V_{L,2}$) generate a negative-time derivative that intends to decrease the active power. That information is being applied to the remaining 11 sectors. This operating is carry on for the reactive power characteristics when the implementation from short ($V_{S,2}$ $V_{S,3}$ $V_{S,4}$), medium ($V_{M,1}$ $V_{M,3}$), long ($V_{L,2}$ $V_{L,3}$ $V_{L,4}$), and zero (V_0 V_7) voltage vectors decide on to deliver a positive time-derivative of reactive power. Then by applying the voltage vectors from short ($V_{S,5}$ $V_{S,6}$), medium ($V_{M,5}$ $V_{M,6}$), and long ($V_{L,5}$ $V_{L,6}$) bring to a negative time-derivative which reduce the reactive power. The same operating has been applied for the remaining 11 sectors in reactive power derivatives. Table 2 presents the new switching table for the three-level NPC AC-DC converter which is developed by analyzing the effect of each four group voltage vector on the changes in active and reactive powers.

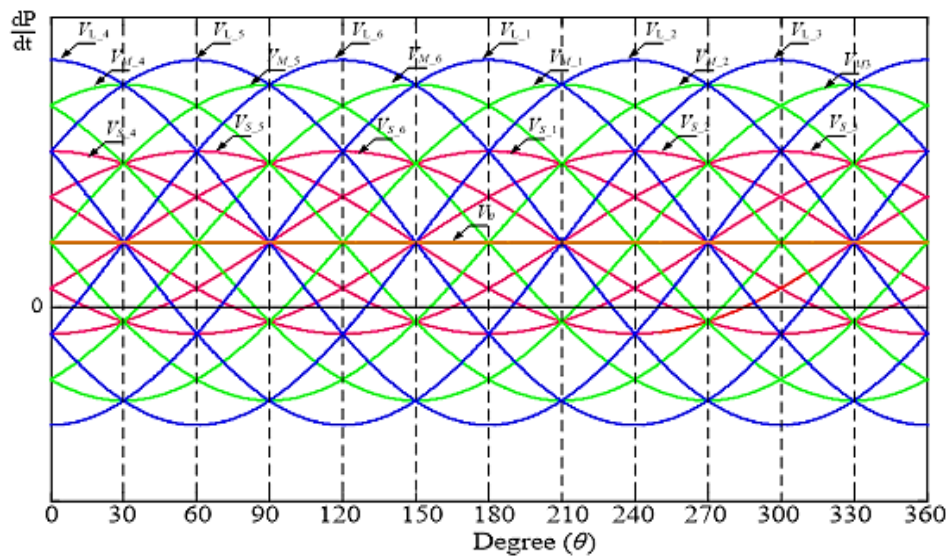


Figure 4. Active power different characteristics under different voltage vector V_n

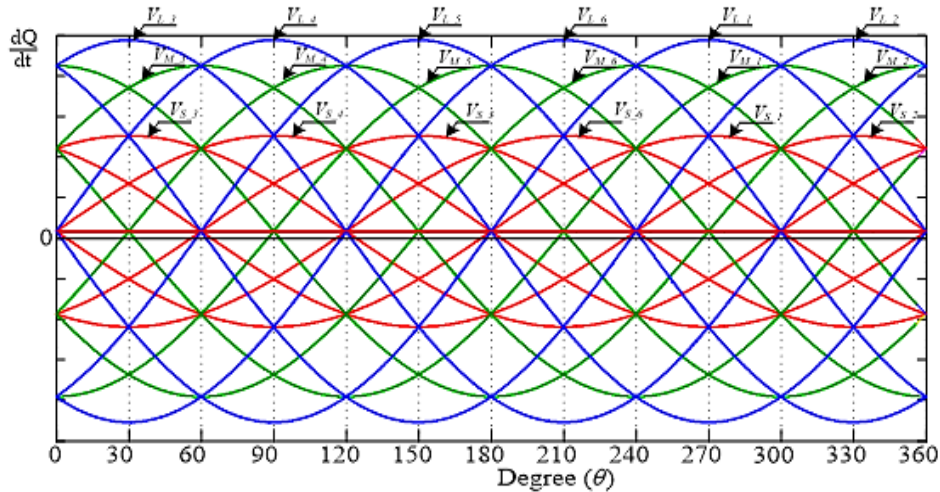


Figure 5. Reactive power differentiation characteristics under different voltage vector V_n

Table 2. New switching table for the 3L-NPC rectifier

Power error status			Sector position (θ_n) and converter voltage vector (V_n)											
d_P	d_Q	B_S	θ_1	θ_2	θ_3	θ_4	θ_5	θ_6	θ_7	θ_8	θ_9	θ_{10}	θ_{11}	θ_{12}
0	0	-	V_{L-1}	V_{M-1}	V_{L-2}	V_{M-2}	V_{L-3}	V_{M-3}	V_{L-4}	V_{M-4}	V_{L-5}	V_{M-5}	V_{L-6}	V_{M-6}
0	1	-	V_{M-1}	V_{L-2}	V_{M-2}	V_{L-3}	V_{M-3}	V_{L-4}	V_{M-4}	V_{L-5}	V_{M-5}	V_{L-6}	V_{M-6}	V_{L-1}
1	0	-	V_{S-5}	V_{S-5}	V_{S-6}	V_{S-6}	V_{S-1}	V_{S-1}	V_{S-2}	V_{S-2}	V_{S-3}	V_{S-3}	V_{S-4}	V_{S-4}
		1	OOP	OOP	POP	POP	POO	POO	PPO	PPO	OPO	OPO	OPP	OPP
		0	NNO	NNO	ONO	ONO	ONN	ONN	OON	OON	NON	NON	NNO	NNO
1	1	-	V_{S-4}	V_{S-4}	V_{S-5}	V_{S-5}	V_{S-6}	V_{S-6}	V_{S-1}	V_{S-1}	V_{S-2}	V_{S-2}	V_{S-3}	V_{S-3}
		1	OPP	OPP	OOP	OOP	POP	POP	POO	POO	PPO	PPO	OPO	OPO
		0	NNO	NNO	NNO	NNO	ONO	ONO	ONN	ONN	OON	OON	NON	NON

* B_S = Balancing status

4. SIMULATION RESULTS

The MATLAB/Simulink software is used to test the effectiveness and performance of the proposed new switching look-up table for 3L-NPC DPC. Table 2 shows the parameters used in 3L-NPC rectifier. In the MATLAB/Simulink model, the appropriate value of inductances and capacitances is set in the range of 11 to 15 mH. In DPC, high gain of controller necessitates the use of inductors with high value [13]. Then, in sample time of the system plays a crucial role in implementation since too large sample times reduce the performance of the system whereas too small sample times increase the burden on the controller. Therefore, when duty cycle control-based techniques are used [16], the sampling frequency can be further reduced to 20 kHz. Figures 6(a) and (b) show that the new switching table can produce a balanced three-phase voltage and line current waveforms, respectively during steady-state conditions. Figure 6(c) represents the unity power factor operation where the phase a voltage and current are in phase. Meanwhile, the estimated instantaneous active power P_{inst} and reactive powers Q_{inst} are shown in Figure 6(d). It is clear to see that the reactive power Q is kept at 0 var to achieve unity power factor operation. The DC output voltage V_{DC} follows the DC reference which is set to 150 V as shown in Figure 6(e). In addition, the THD of the input current is 1.21% which complies with the specification of *IEEE-519* where the current THD should be less than 6% as shown in Figure 6(f). As stated in [5] in FFT analysis, the number of THD has been established by 2.48%. By applying the new method in switching strategy for 3L-NPC DPC the number of THD produced is improved to 1.21%.

The control method is also evaluated under the transient response during load variation. In this case, a 100 Ω resistor is connected in parallel with the existing resistor across the DC-link at 3s to create a sudden disturbance to the load current. A breaker is used in the simulation for connecting the additional resistor to the existing resistor. Figures 7(a)-(c) show the results for a transient response during a load variation. It is apparent to see that the DC output voltage is experiencing a sudden drop with a small dip but it recovers to the original value 150 V forced by the voltage PI regulator. Then, in Figure 7(c) the estimated active power (P) follows the change in load as it increases suddenly at 3s due to the load disturbance. Meanwhile, the overshoot and oscillation are not obvious for reactive power (Q). Lastly, at the time of 3s the line current waveform from phase 'a' started to increase once the disturbance occurs at the time of 3s regarding the

relationship of current and resistance in ohm's law. Next, Figure 7(d) shows the transient response when the DC voltage reference command changes from 150 V to 180 V at 5s and back to 150 V at 8s. With the calculated quantities of the DC-link voltage PI regulator, the DC output voltage V_{DC} follows the V_{DCref} with less overshoot as shown in Figure 7(e). The estimated active power also increases and decreases rapidly to new values during the step changes of the output voltage while keeping the reactive power at 0 var. Lastly, the line current I_a is increased and decreased as shown in Figure 7(f) which accommodates the increasing and decreasing of the converter DC output voltage.

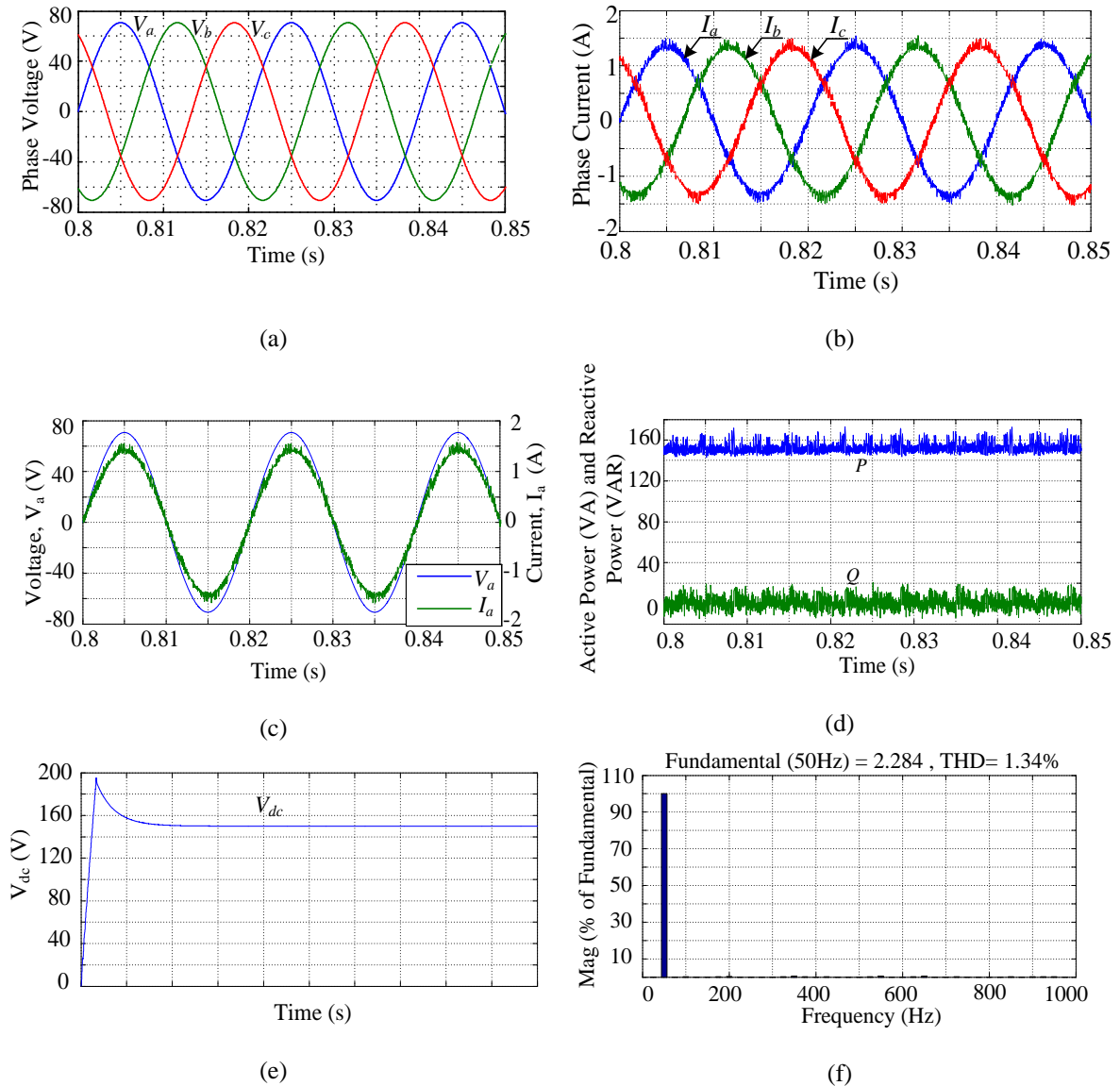


Figure 6. New switching look-up table for 3L-NPC DPC. (a) three-phase supply voltage; (b) three-phase input current; (c) phase a voltage and current at unity power factor operation; (d) estimated input instantaneous active and reactive power at unity power factor operation; (e) generated DC-link output voltage; (f) harmonic spectrum of the input line current

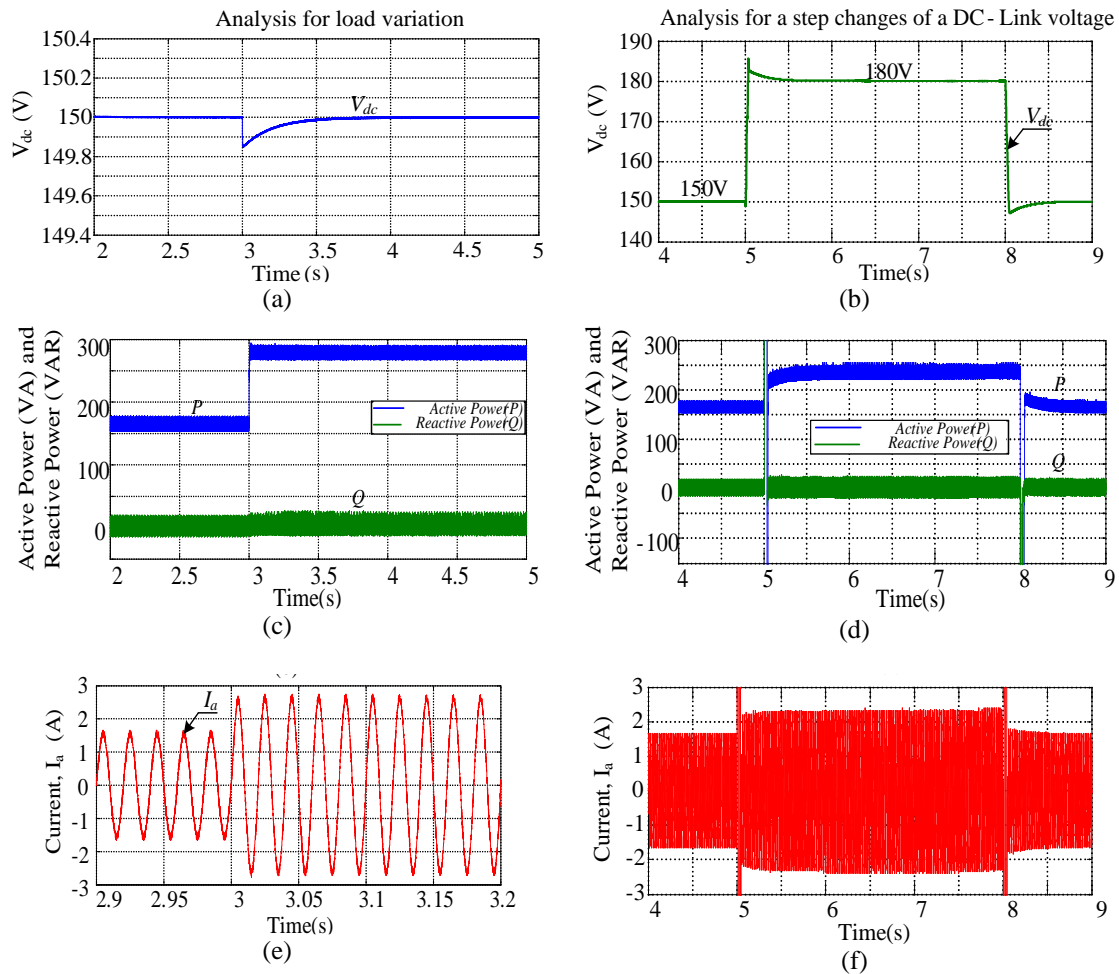


Figure 7. Effectiveness and performance of the proposed new switching look-up table for 3L-NPC DPC. (a)-(c) Transient response for load variation from low to high power demand, and (d)-(f) Transient response for DC output voltage changes; (a) and (d) DC-link output voltage; (b) and (e) Estimated active and reactive power; (c) and (f) Phase 'a' current

5. CONCLUSION

In this paper, a new DPC switching strategy in three-level neutral point clamped (3L-NPC) is introduced. The synthesizing of a new NPC-DPC switching table allows the selection of the best converter voltage vector among all the possible voltage vectors to fulfill the requirement of the converter system instantaneous active and reactive power. The MATLAB/Simulink is used to analyze the effectiveness and performance of the new switching table of DPC.

ACKNOWLEDGMENT

The authors would like thank to the Ministry of Higher Education Malaysia (MOHE), Universiti Teknikal Malaysia Melaka (UTeM) for providing the research grant of PJP/2017/FKE/HI12/S01539

REFERENCES

- [1] G. S. Shehu, A. B. Kunya, I. H. Shanono, and T. Yalcinoz, "A Review of Multilevel Inverter Topology and Control Techniques," *International Journal of Automation and Control*, vol. 4, no. 3, pp. 233–241, 2016, doi: 10.18178/joace.4.3.233-241.
- [2] S. Kouro et al., "Recent Advances and Industrial Applications of Multilevel Converters," in *IEEE Transactions on Industrial Electronics*, vol. 57, no. 8, pp. 2553–2580, Aug. 2010, doi: 10.1109/TIE.2010.2049719.
- [3] Bor-Ren Lin, Chi-Nam Wang and Hsin-Hung Lu, "Multilevel AC/DC/AC converter by using three-level boost rectifier and five-level diode clamped inverter," *Proceedings of the IEEE 1999 International Conference on Power*

- Electronics and Drive Systems. PEDS'99 (Cat. No.99TH8475)*, 1999, pp. 444-449 vol.1, doi: 10.1109/PEDS.1999.794604.
- [4] A. F. Okou, M. Tarbouchi, D. Bouchard and A. A. Amoussou, "A New Robust Controller for a Three-Phase Three-Level NPC Rectifier," *IECON 2007 - 33rd Annual Conference of the IEEE Industrial Electronics Society*, 2007, pp. 1755-1761, doi: 10.1109/IECON.2007.4460322.
- [5] N. Li, Y. Wang, S. Li, Y. Li and Z. Wang, "Direct power control strategy used in three-level NPC converters," *Proceedings of The 7th International Power Electronics and Motion Control Conference*, 2012, pp. 1675-1679, doi: 10.1109/IPEMC.2012.6259087.
- [6] H. A. Hamed, A. F. Abdou, M. S. E. Moursi and E. E. EL-Kholly, "A Modified DPC Switching Technique Based on Optimal Transition Route for of 3L-NPC Converters," in *IEEE Transactions on Power Electronics*, vol. 33, no. 3, pp. 1902-1906, March 2018, doi: 10.1109/TPEL.2017.2743230.
- [7] N. Li, N. Zhi, H. Zhang, Y. Wang and Z. Wang, "A novel switching table based direct power control strategy of three-level NPC rectifier," *2016 IEEE 8th International Power Electronics and Motion Control Conference (IPEMC-ECCE Asia)*, 2016, pp. 2378-2381, doi: 10.1109/IPEMC.2016.7512669.
- [8] H. Yin and S. Dieckerhoff, "Experimental comparison of DPC and VOC control of a three-level NPC grid connected converter," *2015 IEEE 6th International Symposium on Power Electronics for Distributed Generation Systems (PEDG)*, 2015, pp. 1-7, doi: 10.1109/PEDG.2015.7223072.
- [9] P. Zolov, N. Poliakov and V. Tomasov, "Carrier Amplitude Control for Neutral Point Balancing in a Multilevel Active Voltage Rectifier," *2018 X International Conference on Electrical Power Drive Systems (ICEPDS)*, 2018, pp. 1-5, doi: 10.1109/ICEPDS.2018.8571883.
- [10] D. Semenov, B. Tian, Li Sun and G. Mirzaeva, "Advanced fault-tolerant current control of five-phase PMSM for mining applications," *2016 IEEE Industry Applications Society Annual Meeting*, 2016, pp. 1-7, doi: 10.1109/IAS.2016.7731918.
- [11] Y. K. Tao, L. Wang, Q. H. Wu and W. H. Tang, "Virtual-flux-based predictive direct power control of three-phase AC/DC converters," *2014 IEEE PES Asia-Pacific Power and Energy Engineering Conference (APPEEC)*, 2014, pp. 1-6, doi: 10.1109/APPEEC.2014.7066109.
- [12] N. A. Mohd Yusoff, A. M. Razali, K. Abdul Karim, A. Jidin, and T. Sutikno, "An Analysis of Virtual Flux Direct Power Control of Three-Phase AC-DC Converter," *International Journal of Power Electronics and Drive Systems*, vol. 9, no. 3, p. 947, 2018, doi: 10.11591/ijpeds.v9.i3.pp947-956.
- [13] A. M. Razali, M. A. Rahman, G. George and N. A. Rahim, "Analysis and Design of New Switching Lookup Table for Virtual Flux Direct Power Control of Grid-Connected Three-Phase PWM AC-DC Converter," in *IEEE Transactions on Industry Applications*, vol. 51, no. 2, pp. 1189-1200, March-April 2015, doi: 10.1109/TIA.2014.2344503.
- [14] S. Venkateshwarlu, B. P. Muni and A. D. Rajkumar, "Analysis of VF-DPC PWM converter based STATCOM," *2008 Annual IEEE India Conference*, 2008, pp. 431-436, doi: 10.1109/INDCON.2008.4768762.
- [15] P. Antoniewicz, and M.P. Kazmierkowski, "Predictive direct power control of three-phase boost rectifier," *Bulletin of the Polish Academy of sciences technical sciences*, vol. 54, no. 3, 2006, p.p.287-292.
- [16] S. Aurtenechea, M. A. Rodriguez, E. Oyarbide and J. R. Torrealday, "Predictive Direct Power Control - A New Control Strategy for DC/AC Converters," *IECON 2006 - 32nd Annual Conference on IEEE Industrial Electronics*, 2006, pp. 1661-1666, doi: 10.1109/IECON.2006.347519.
- [17] Y. Zhang, W. Xie, Z. Li and Y. Zhang, "Model Predictive Direct Power Control of a PWM Rectifier With Duty Cycle Optimization," in *IEEE Transactions on Power Electronics*, vol. 28, no. 11, pp. 5343-5351, Nov. 2013, doi: 10.1109/TPEL.2013.2243846.
- [18] J. Hu and Z. Q. Zhu, "Improved Voltage-Vector Sequences on Dead-Beat Predictive Direct Power Control of Reversible Three-Phase Grid-Connected Voltage-Source Converters," in *IEEE Transactions on Power Electronics*, vol. 28, no. 1, pp. 254-267, Jan. 2013, doi: 10.1109/TPEL.2012.2194512.
- [19] A. Mehdi, S. E. Rezgui, H. Medouce, and H. Benalla, "A comparative study between DPC and DPC-SVM controllers using dSPACE (DS1104)," *International Journal of Electrical and Computer Engineering*, vol. 4, no. 3, pp. 322-328, 2014, doi: 10.11591/ijece.v4i3.6074.
- [20] M. Malinowski, M. Jasinski and M. P. Kazmierkowski, "Simple direct power control of three-phase PWM rectifier using space-vector modulation (DPC-SVM)," in *IEEE Transactions on Industrial Electronics*, vol. 51, no. 2, pp. 447-454, April 2004, doi: 10.1109/TIE.2004.825278.
- [21] L. Xiao, S. Huang, T. Liu, Q. Xu and K. Huang, "A novel SVM-DPC control method for grid connected AC-DC converters under asymmetrical fault," *2011 International Conference on Power Engineering, Energy and Electrical Drives*, 2011, pp. 1-6, doi: 10.1109/PowerEng.2011.6036496.
- [22] Y. Wang, A. Aksoz, T. Geury, S. B. Ozturk, O. C. Kivanc, and O. Hegazy, "A review of modular multilevel converters for stationary applications," *Applied Sciences*, vol. 10, no. 21, pp. 1-36, 2020, doi: 10.3390/app10217719.
- [23] R. Teichmann and S. Bernet, "A comparison of three-level converters versus two-level converters for low-voltage drives, traction, and utility applications," in *IEEE Transactions on Industry Applications*, vol. 41, no. 3, pp. 855-865, May-June 2005, doi: 10.1109/TIA.2005.847285.
- [24] S. Rivera et al., "Generalized direct power control for grid connected multilevel converters," *2010 IEEE International Conference on Industrial Technology*, 2010, pp. 1351-1358, doi: 10.1109/ICIT.2010.5472518.
- [25] M. Lu, J. Hu, R. Zeng, W. Li and L. Lin, "Imbalance Mechanism and Balanced Control of Capacitor Voltage for a Hybrid Modular Multilevel Converter," in *IEEE Transactions on Power Electronics*, vol. 33, no. 7, pp. 5686-5696, July 2018, doi: 10.1109/TPEL.2017.2743780.